Latest results of the OPERA Neutrino Experiment

M. S. Vladymyrov[a*]
On behalf of the OPERA Collaboration
[a] *Lebedev Physical Institute, 119991, Moscow, Leninsky prsp. 53*

Abstract

The OPERA neutrino experiment in the underground Gran Sasso Laboratory (LNGS) was designed to perform the first detection of neutrino oscillations in direct appearance mode in the $\nu_\mu \to \nu_\tau$ channel, the ν_τ signature being the identification of the τ-lepton created in its charged current interaction. The hybrid apparatus consists of a large mass emulsion film/lead target complemented by electronic detectors. Placed in the LNGS, it is exposed to the high-energy long-baseline CERN Neutrino beam to Gran Sasso (CNGS) 730 km away from the neutrino source. The observation of a first ν_τ candidate event was reported in 2010. In this paper, we discuss the result of the analysis of the data taken during the first two years of operation $(2008 - 2009)$ underlining the major improvements brought to the analysis chain and to the Monte Carlo simulations. The statistical significance of the one event observed so far is then evaluated to 95%. Also we report about a second ν_τ candidate event found in the 2010-2011 data sample which processing is going on. The electron neutrino search procedure is described. Finally we give the latest results on the neutrino velocity measurement in the CNGS beam.

1 Introduction

Neutrino oscillations were first predicted nearly 50 years ago [1] and were definitely established in 1998 by the super-Kamiokande experiment with atmospheric neutrinos [2]. Several other experiments carried out in the last two decades with atmospheric, solar, reactor and accelerator neutrinos have established our current understanding of neutrino mixing and oscillations (see e.g. for a review [3]). In particular, the depletion in the ν_μ neutrino flux through oscillation observed by several atmospheric neutrino experiments [2, 4] was confirmed by two accelerator experiments [5]. The fact that the $\nu_\mu \to \nu_e$ oscillation cannot be the dominant channel has been indirectly confirmed by two nuclear reactor experiments [6]. An indication of the appearance of ν_e in a ν_μ beam with a statistical significance of 2.5σ has recently been published by the T2K experiment [7]. The appearance of ν_τ in an accelerator ν_μ beam will unambiguously prove that $\nu_\mu \to \nu_\tau$ oscillation is the dominant transition channel for the neutrino atmospheric sector. This is the main goal of the long-baseline OPERA experiment [8, 9], with its detector exposed in the Gran Sasso underground laboratory (LNGS) to the high-energy CERN CNGS neutrino beam [10].

The detection of CNGS neutrino interactions in OPERA was reported in [11] and the observation of a first ν_τ candidate event was presented in [12]. In this paper, we summarize the major improvements brought to the analysis chain and to the Monte Carlo simulations. They mainly concern the evaluation of the efficiencies and the reduction or better control of the physics backgrounds. Event statistics acquired during the first two years of data-taking in 2008 and 2009 and corresponding to 4.88×10^{19} protons on target (p.o.t.) are used for the studies reported here. The statistical significance of the observation of one ν_τ candidate event reported in [12] is re-assessed.

* **e-mail**: neworldemancer@gmail.com

2 The OPERA detector and the CNGS beam

The challenge of the OPERA experiment is to achieve the very high spatial accuracy required for the detection of τ leptons (whose decay length is of the order of 1mm in this experiment) inside a large-mass active target. The hybrid detector [13] is composed of two identical super modules (SM), each consisting of an instrumented target section of a mass of about 625 tons followed by a magnetic muon spectrometer. A target section is a succession of walls filled with elements called bricks, interleaved with planes of scintillator strips composing the target tracker (TT) that triggers the read-out and allows localizing neutrino interactions within the target. A brick is an emulsion cloud chamber module consisting of 56 1-mm-thick lead plates interleaved with 57 nuclear emulsion films. It weighs 8.3 kg and its thickness corresponds to ten radiation lengths along the beam direction. Tightly packed removable doublets of emulsion films called changeable sheets (CS) are glued to the downstream face of each brick. They serve as interfaces between the TT planes and the bricks to facilitate the location of neutrino interactions. Large brick-handling ancillary facilities are used to bring emulsion films from the target up to the automatic scanning microscopes in Europe and Japan. Extensive information on the OPERA detector and facilities is given in [13, 14, 15].

OPERA is exposed to the long-baseline CNGS ν_μ beam [10], 730 km away from the source. The beam is optimized for the observation of ν_τ CC interactions. The average neutrino energy is 17 GeV. In terms of interactions, the $\bar{\nu_\mu}$ contamination is 2.1%, the ν_e and $\bar{\nu_e}$ contaminations are together lower than 1%, while the intrinsic ν_τ component in the beam is negligible.

3 Location of neutrino interactions

The expected number of neutrino events registered in the target volume is 850 per 10^{19} protons on target (p.o.t.) per 1000 tons. A 10% error is assigned to this number resulting from uncertainties on the neutrino flux and interaction cross-sections. During the 2008 and 2009 runs, the average target mass was 1290 tons, of which 8.6% was dead material other than lead plates and emulsion films. The total number of p.o.t was 1.78×10^{19} in 2008 and 3.52×10^{19} in 2009, respectively.

With a trigger efficiency of 99%, the total numbers of triggers in 2008 and 2009 ontime with the beam amount to 10 121 and 21 455, respectively. About 85% of these are due to particles entering the target after being emitted in neutrino interactions occurring in the rock surrounding or in material inside the LNGS cavern. This component, hereafter called external events, was identified during the 2008 run by performing a visual inspection of all on-time events. Events with topologies consistent with charged particles entering the detector or with low-energy interaction of neutrons and γ-rays, mimicking a neutral current (NC) interaction, were discarded from the sample. For the 2008 data, stringent criteria were used, guaranteeing a high level of purity at the cost of some inefficiency for very low activity events. A total of 1698 events was retained and constitutes the 2008 sample. In 2009, events compatible with occurring in the target volume were selected by an automatic algorithm [16, 17] developed on the basis of the experience acquired with the 2008 sample. The automatic procedure reduces the human workload required by the visual inspection. It also aims at reaching higher efficiency for a specific category of signal events: τ emitted in quasi-elastic (QE) interactions decaying to an electron have a topology very similar to external NC-like events. The drawback is an increased number of external events to be measured.

A Monte Carlo simulation including both external events and interactions occurring inside the target well reproduces the experimental data for what concerns the event rates and position distribution inside the target, validating the automatic selection algorithm. This is particularly true for the low-energy external NC-like events which accumulate close to the target borders. The efficiency of the algorithm is estimated by simulation to be 96.2 and 86.3% for CC and

NC events, respectively. The contamination by external events, lower than 1% for CC events, is 23.3% for NC events. By applying the automatic selection algorithm on the 2009 sample, 3629 events were expected from the simulation and 3693 were eventually retained from the experimental data. The sample was further reduced to 3557 events after visual inspection of the event displays.

Data from the electronic detectors associated with the 5255 events reconstructed as occurring inside the target volume were processed by a software algorithm that selects the brick with the highest probability to contain the neutrino interaction vertex. The brick so designated is removed from the target, the CS is detached and its films are searched for tracks compatible with the electronic data to verify the brick selection. In the case this search is unsuccessful, the brick is equipped with a fresh CS and reinserted into the target. A second brick is then extracted according to its probability to contain the vertex complemented by a visual inspection of the event display. In the case the search is successful the brick is dismounted and the emulsion films are dispatched to the scanning laboratories. All tracks measured with high precision in the CS films are sought in the most downstream films of the brick. These tracks are then followed back until they are not found in three consecutive films. A volume is then scanned around their stopping point in order to localize the interaction vertex.

4 Search for decay topologies: the observation of ν_τ candidate events

Preserving a high selection efficiency for the QE $\tau \rightarrow e$ channel at the cost of a larger contamination of external events does not increase significantly the number of interaction vertices located in the target (consisting mainly of ν_μ CC and NC events). This number can therefore be predicted by relying only on the size of the essentially uncontaminated 2008 sample. From the 1698 events constituting the 2008 sample, a fraction of about 5% of the events was rejected because of occurring in bricks equipped with poor-quality emulsion films, 1000 interaction vertices were located in bricks and 110 in the dead material. The resulting vertex location efficiencies are 74 ± 2 and 48 ± 4% for CC and NC ν_μ interactions, respectively. By rescaling for the integrated p.o.t., the expected number of located events to be searched for decays of short-lived particles in the entire 2008 and 2009 samples is 2978 ± 75. More information on detection efficiencies for signal events is given in section 5. The results presented in this paper concern the decay search analysis of 2738 events, i.e. 92% of the total 2008 and 2009 event sample. The bias on efficiency estimations the lack of the remaining 8% of events may induce, if any, is negligible. In the analysed sample, which corresponds to a total of 4.88×10^{19} p.o.t., 81% of events have an identified muon in the final state.

In order to analyse the primary vertex a volume scan is performed over a 1 cm^2 area in at least two films upstream and six films downstream of the vertex lead plate. A procedure was developed to detect charged and neutral decays as well as secondary interaction and γ-ray conversion vertices in the vicinity of the primary vertex; it was introduced in [12] and detailed in [18].

When a secondary vertex is found the kinematical analysis of the whole event is performed. This analysis uses the values of the angles measured in the emulsion films, of the momenta determined by multiple Coulomb scattering measured in the brick, of the momenta measured by the magnetic spectrometers and of the total energy deposited in the instrumented target acting as a calorimeter [12, 17, 19]. The energy of γ-rays and electrons is estimated by a neural network algorithm that uses the combination of the number of track segments in the emulsion films and the shape of the electromagnetic shower, together with the multiple Coulomb scattering of the leading tracks. By applying this procedure, one ν_τ candidate event was observed, as reported in detail in [12]. We recall that the tau-candidate event had seven prongs at the primary vertex, out of which four are identified as originating from a hadron and three have a probability lower than 0.1% of being caused by a muon, none being left by an electron. The parent track exhibits a kink topology and the daughter track is identified as produced by a hadron through its interaction. Its impact parameter with respect to the primary vertex is $(55 \pm 4)\mu m$; the impact parameter is smaller than $7\mu m$ for the other tracks. Two γ-rays point to the secondary vertex. The event passes all the selection cuts defined in the experiment proposal and summarized in table 1 [9].

Table 1: Selection criteria for ν_τ candidate events as set in [9] and the corresponding values measured for the first observed tau-candidate event [12].

Variable	Cut-off	Value
Missing p_T at the primary vertex (GeV/c)	< 1.0	$0.57^{+0.32}_{-0.17}$
Angle between the parent track and the primary hadronic shower in the transverse plane (rad)	$> \pi/2$	3.01 ± 0.03
Kink angle (mrad)	> 20	41 ± 2
Daughter momentum (GeV/c)	> 2	12^{+6}_{-3}
Daughter p_T when γ-ray at the decay vertex (GeV/c)	> 0.3	$0.47^{+0.24}_{-0.12}$
Decay length (μm)	$<$ 2 lead plates	1335 ± 35

The invariant mass of the two γ-rays is $(120 \pm 20(stat.) \pm 35(syst.))MeV/c^2$, consistent with the π^0 mass. Together with the secondary hadron assumed to be a π^- they have an invariant mass of $(640^{+125}_{-80}(stat.)^{+100}_{-90}(syst.))MeV/c^2$. The decay mode is therefore compatible with being $\tau \to \rho^-(770)\nu_\tau$, whose branching ratio is about 25%. The statistical significance of this event was estimated to be 98.2%, as the probability that it was not due to a fluctuation of the background simulating a decay in the $\tau \to h$ channel [12].

Processing of the 2010-2011 data is going on and recently in this sample a second ν_τ was observed. The event topology is shown on figure 1. It has 2 prongs at the primary vertex and one nuclear fragment. A first primary vertex track is found to be a hadron. It stops after two brick walls downstream. The other primary vertex track decays into 3 tracks, no nuclear fragments are present. One of the daughter particles decays 1.3 cm downstream into 2 daughter tracks and four nuclear fragments which originate from this second decay vertex. The average kink angle found is 87.4 mrad. The total momentum of daughters is $8.4 \pm 1.7GeV/c$. The event passes all the selection cuts defined in the experiment proposal for $\tau \to 3h$ events which are summarized in table 2.

Table 2: Selection criteria for ν_τ candidate event in $\tau \to h$ chanel as set in [9] and the corresponding values measured for the second tau-candidate event.

Variable	Cut-off	Value
Angle between the parent track and the primary hadronic shower in the transverse plane (rad)	$> \pi/2$	2.929 ± 0.019
Avrage kink angle (mrad)	< 500	87.4 ± 1.5
Total momentum at secondary vertex (GeV/c)	> 3.0	8.4 ± 1.5
Minimal incariant mass (GeV/c^2)	$> 0.5and < 2.0$	0.80 ± 0.12
Transverse momentum at the primary vertex (GeV/c)	< 1.0	0.31 ± 0.11
Decay length (μm)	$<$ 2 lead plates	1540 ± 50

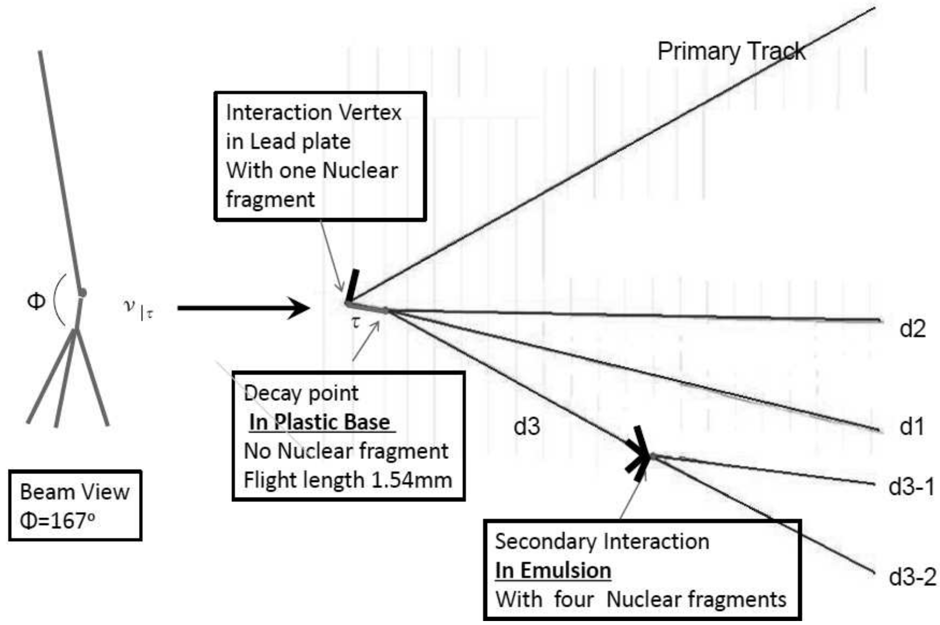

Figure 1: Second ν_τ candidate event topology

5 Signal detection efficiencies and physics background

The validity of the Monte Carlo simulation of the electronic detectors response has been verified through a detailed comparison with experimental data. This comparison concerns the muon identification and the reconstruction of its momentum and charge, as well as the reconstruction of the total energy and the hadronic shower profile [17]. The event simulation and the off-line reconstruction software have been extended to the response of the emulsion films, allowing all the algorithms used in the analysis of real events to be applied to simulated data. This includes scanning of the CS films, track connection between CS films and downstream films of the brick and track following towards the vertex. The subsequent scan of a volume around the vertex is complemented by track following from the vertex and searching for secondary decay or interaction vertices and for electromagnetic showers [20]. Simulation and off-line reconstruction algorithms have been successfully implemented up to the events topology and their location inside the bricks. The agreement between experimental and simulated data is shown in figures 2 and 3. Further work is in progress with the aim of a full, data-driven simulation of all scanning and analysis phases.

Charged charmed particles have lifetimes similar to that of the τ lepton and share analogous decay topologies. The finding efficiency of the decay vertices is therefore also similar for both types of particles. Comparing the observed charm event sample in size, decay topologies and kinematics with expectations from simulations constitutes a straightforward way to verify that prompt-decay selection criteria and their corresponding efficiencies and backgrounds are well understood. Recently published cross-sections have been used in the simulation [20]. The results of this comparison are shown in table 3. Figure 4 shows the distributions of the decay length and of the angle ϕ between the parent track and the primary muon in the plane transverse to the beam direction. There is good agreement between experimental and simulated data both in the number of expected charm events and in the quoted distributions.

The expected numbers of events in the various τ channels for the nominal beam intensity of 22.5×10^{19} p.o.t. in 5 years foreseen in the experiment proposal [9] and for the fraction of the 2008 and 2009 runs analysed so far are shown in table 3. Full mixing and $\Delta m^2_{23} = 2.5 \times 10^{-3} eV^2$ are assumed. The total number of signal events expected to be eventually detected decreased

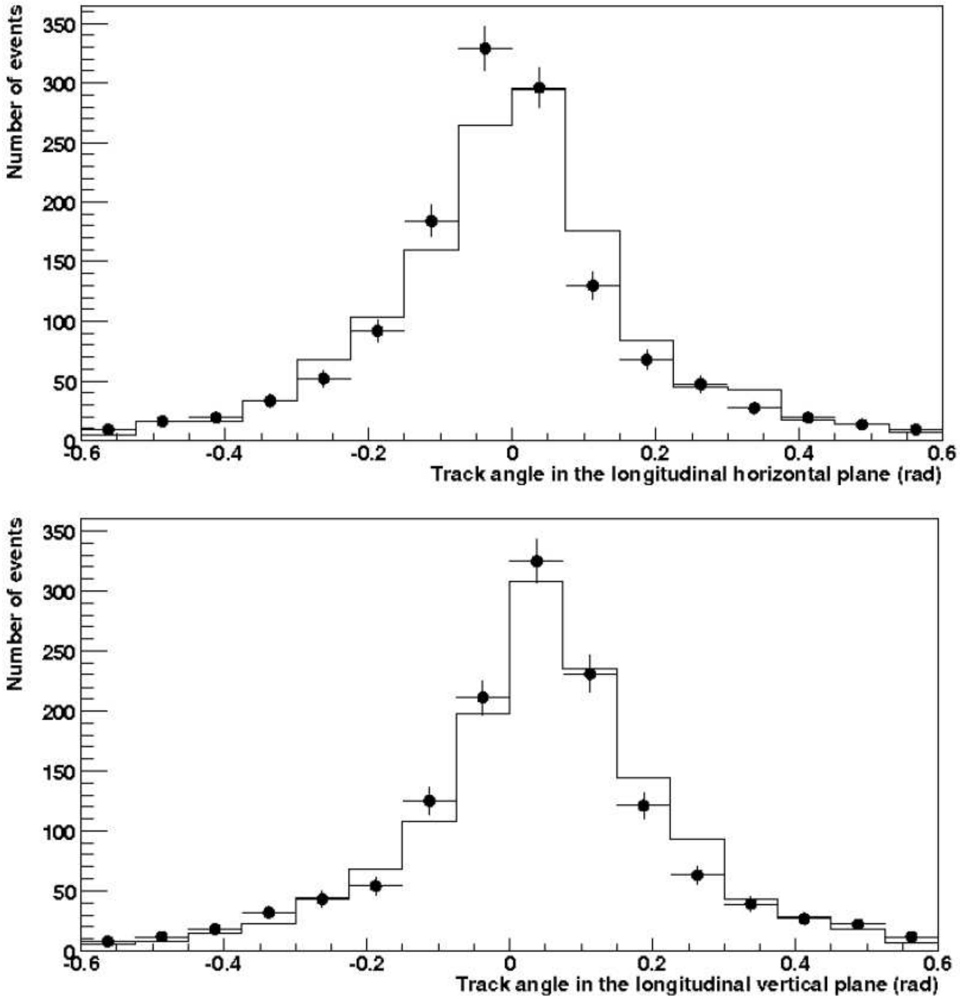

Figure 2: Angle of tracks reconstructed at the primary vertex in the longitudinal horizontal (top) and vertical (bottom) planes: comparison between experimental data (lines with error bars) and simulated data (continuous line).

Table 3: Comparison of charm event topologies observed and expected from simulations including background.

Topology	Observed charm candidate events	Expected events		
		Charm	Background	Total
Charged one-prong	13	15.9	1.9	17.8
Neutral two-prong	18	15.7	0.8	16.5
Charged three-prong	5	5.5	0.3	5.8
Neutral four-prong	3	2.0	< 0.1	2.1
Total	39	39.1 ± 7.5	3.0 ± 0.9	42.2 ± 8.3

from about 10 as quoted in the experiment proposal [9] to 8, essentially because of the reduced interaction vertex location efficiencies resulting from a more reliable knowledge of the detector and of the analysis procedures. These updated interaction vertex location efficiencies are shown in table 4 together with the global τ detection efficiency that includes the interaction and decay vertices detection efficiencies as well as the selection efficiency to satisfy topological and kinematical criteria at both vertices.

The main source of background to all τ-decay channels is the charged charmed particles that

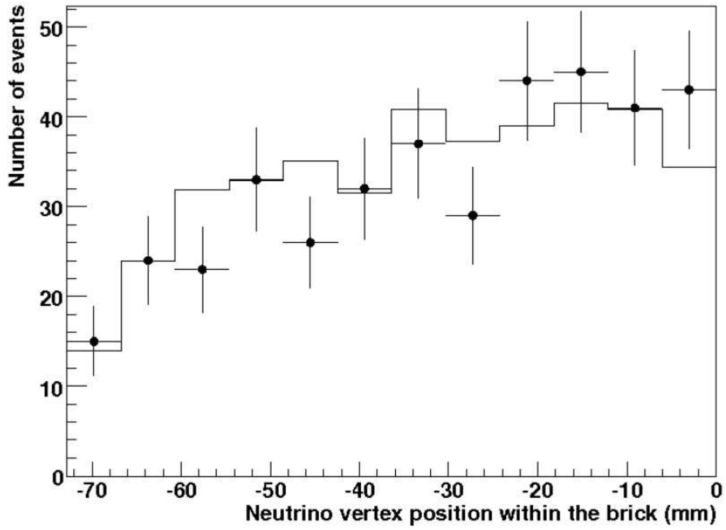

Figure 3: Location within the bricks of the primary vertex of NC events: comparison between experimental data (dots with error bars) and simulated data (continuous line). Most ν_τ CC events have topologies similar to NC events.

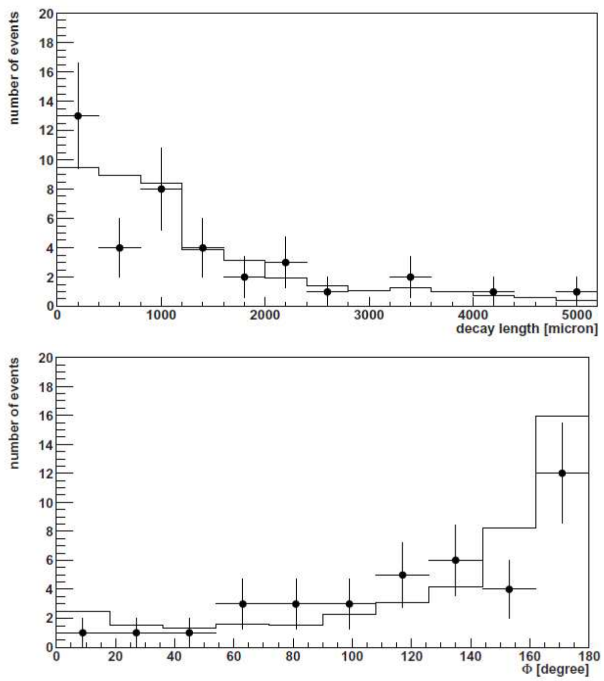

Figure 4: Top: distributions of the decay length of charmed particles for experimental data (dots with error bars) and simulated data (histogram). Bottom: distributions of the angle ϕ between the parent track and the primary muon in the transverse plane of charmed particles for experimental data (dots with error bars) and simulated data (histogram).

decay into similar channels and are produced in ν_μ CC interactions where the primary muon is not identified. However, the charmed muon decay channel does not contribute to background if the opposite sign muon charge is correctly measured by the spectrometers. Additional charm background can arise from $c\bar{c}$ pair production in NC interactions where one charmed particle is not identified, and from $\bar{\nu_\mu}$, ν_e and $\bar{\nu_e}$ CC events that amount to 2.5% in terms of interactions. Second-order effects result from the misidentification of the decay products and the topology.

Table 4: Expected numbers of observed signal events for the design intensity of 22.5×10^{19} p.o.t. and for the 2008 and 2009 analysed data sample corresponding to 4.88×10^{19} p.o.t. The updated efficiency for locating interaction vertices is shown in the fourth column. The last column shows the global τ-detection efficiency that includes detection and selection efficiencies for both interaction and decay vertices as well as the probability to satisfy topological and kinematical criteria at both vertices.

Decay channel	Number of signal events expected for $22.5 \times 10^{19} p.o.t.$	$4.88 \times 10^{19} p.o.t.$	Interaction vertex location efficiency	Global τ detection efficiency
$\tau \to \mu$	1.79	0.39	0.54	0.09
$\tau \to e$	2.89	0.63	0.59	0.14
$\tau \to h$	2.25	0.49	0.59	0.04
$\tau \to 3h$	0.71	0.15	0.64	0.04
Total	7.63	1.65	0.59	0.07

Identifying the muons coming from the primary vertex with the highest possible efficiency is important for suppressing background. Details of muon identification algorithms based on signals collected by the electronic detectors can be found in [17]; 95% efficiency is reached for the primary muons of charm events. In order to further reduce the muon identification inefficiency, all tracks at the primary interaction of signal candidate events emitted with a polar angle θ smaller than 1 rad are followed within the brick in which the event occurs and from brick to brick. About 30% of muons not identified by the electronic detectors are recovered through the topology of their end-point, range-momentum correlation and energy loss measurement in the last fraction of their range. The residual inefficiency is dominated by muons emitted at angles larger than 1 rad or escaping the target from the side. The technique, in particular, allows a sizable reduction of the background in the $\tau \to \mu$ channel due to wrong associations of the muons emitted in ν_μ CC events to the vertex of secondary hadronic interactions with kink topologies. This is also true for fake muons in NC events. The hadronic background is also lowered in the $\tau \to h$ channel due to hadron interactions with kink topologies at the primary vertex of ν_μ CC events where the primary muon has escaped identification in the electronic detectors. The technique had been applied in the analysis of the first ν_τ candidate event but not taken into account in the background estimate since the simulation required for assessing it was not available at that time.

The charm background was evaluated using the charm production cross-sections recently published by the CHORUS Collaboration [21]; they are significantly larger than those known at the time of the experiment proposal [9]. The charm production rate induced by neutrinos relative to the CC cross-section is 35% higher at OPERA energies, while the relative charm fragmentation fraction into D^+ increased from 10 to 22%. The overall effect is a charm background increase by a factor of 1.6-2.4 depending on the decay channel.

The second main source of background in the $\tau \to h$ decay channel comes from one-prong inelastic interactions of primary hadrons produced in NC interactions, or in CC interactions where the primary lepton is not identified and in which no nuclear fragments can be associated with the secondary interaction. This has been evaluated with a FLUKA [22]-based Monte Carlo code, as detailed in [12] and cross-checked with three sets of measurements.

Tracks of hadrons from neutrino interactions have been followed far from the primary vertex over a total length of 14 m; this corresponds to the total length of tracks left by hadrons in 2300 NC events. No interactions have been found that fulfil the $\tau \to h$ selection criteria. Immediately outside the signal region, 10 single-prong interactions have been observed with a p_T larger than 200MeV/c, while 10.8 were expected from simulations. On the top part of figure 5 the total momentum is plotted versus the transverse momentum of the final state particles for these interactions. The parameters space in which τ-decay candidates are accepted is shown.

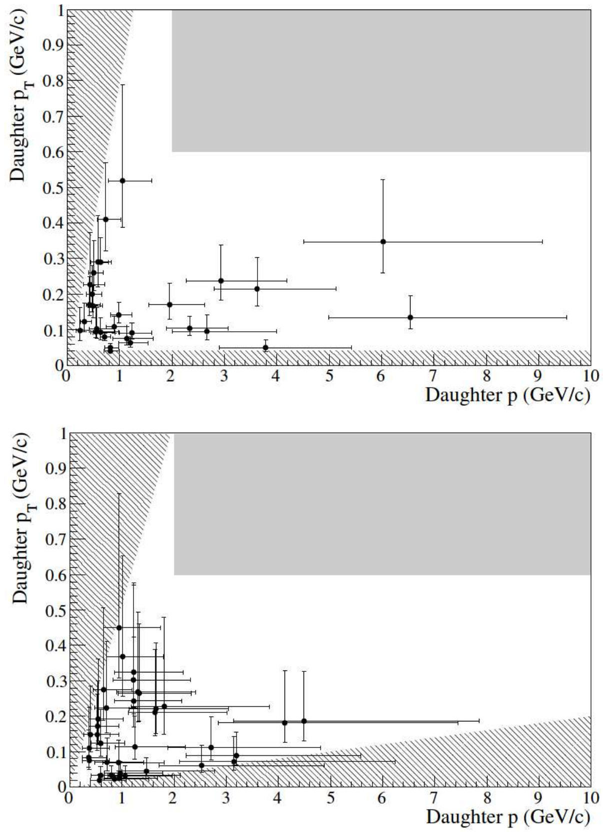

Figure 5: Top: scatter plot of p_T versus p of the daughter particle of single-prong re-interactions of hadrons far from the neutrino interaction vertices where they are produced. Bottom: scatter plot of p_T versus p of the daughter particle of single-prong interactions of 4 GeV/c π^-. On both figures the dark area defines the domain in which τ decay candidates are selected and the hatched area defines the non-physical region $p < p_T$ and the domain rejected by the selection cuts.

OPERA-like bricks exposed to 4 GeV/c π^- beams have been analysed in order to further crosscheck the estimate of the hadron interaction background. In a first exposure, 314 interactions were localized with an angular acceptance $\theta < 1$ rad, out of which 140 are single-prong events with a kink angle larger than 20 mrad (the same selection cut as for the τ decay search). In a second exposure, 314 interactions were located with an angular acceptance $\theta < 0.54$ rad, out of which 126 are single-prong events with kink angles larger than 20 mrad. On the bottom part of figure 5 the transverse momentum is plotted against the total momentum of the final state particles for the single-prong events in this second exposure. Comparisons showing fair agreement between experimental and simulated data of both exposures are presented in figure 6 for a set of topological variables.

The hadron interactions background can be further reduced by increasing the detection efficiency of highly ionizing particles, low-energy protons and nuclear fragments, emitted in the cascade of intra-nuclear interactions initiated by the primary particles and in the nuclear evaporation process. This is a novel feature not yet implemented in the analysis reported in [12]. In order to detect a significant fraction of nuclear fragments emitted at large angle, an image analysis tool was developed. High-resolution microscope tomographic images in 24 layers of 2.5mm×2.1mm size are analysed in the upstream and downstream films of an interaction vertex. This technique was applied to a sample of 64 interactions in an OPERA-like brick exposed to an 8 GeV/c π^- beam. At least one highly ionizing particle was associated with $(56 \pm 7)\%$ of the events with a backward/forward asymmetry of 0.75 ± 0.15, while 53% are

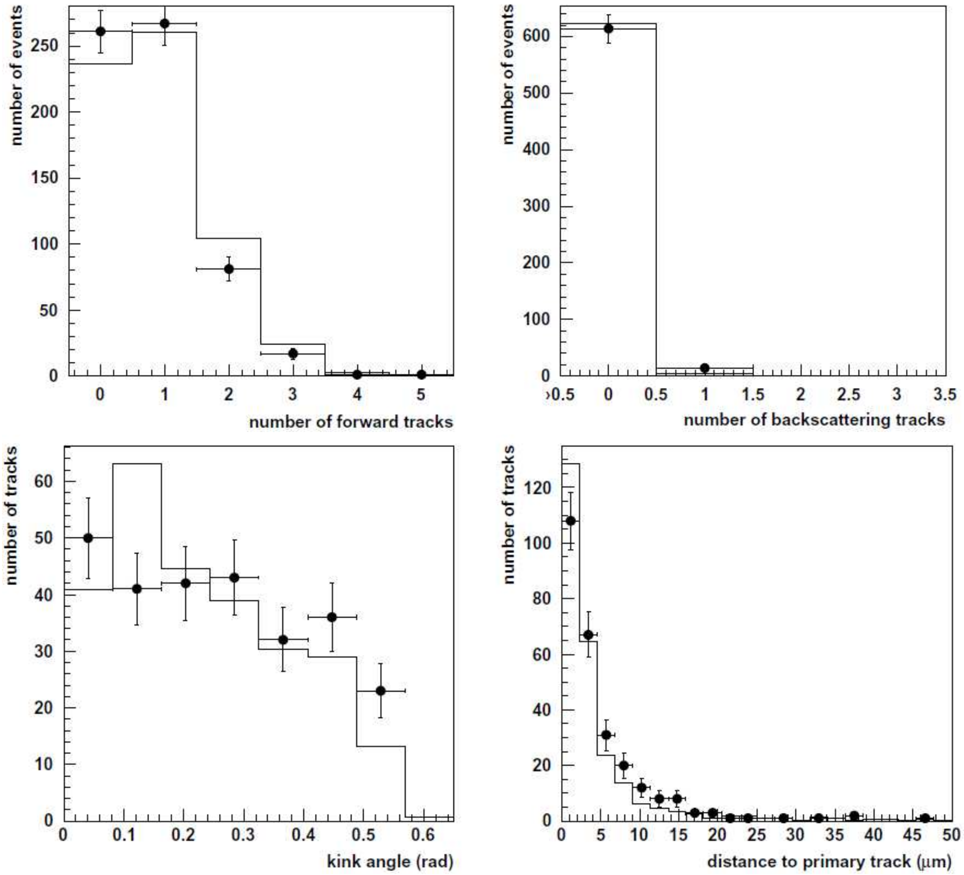

Figure 6: Comparison of experimental data (dots with error bars) and simulation data (histogram) for two bricks exposed to 4 GeV/c π^- test beams. Normalizations are independent. Top left: forward tracks multiplicity. Top right: backward tracks multiplicity. Bottom left: kink angle for one-prong events. Bottom right: minimum distance between the primary and the secondary tracks for one-prong events.

expected from simulations with an asymmetry of 0.71. Figure 7 shows fair agreement in polar angle distribution of the highly ionizing particles between experimental and simulated data. The technique allows detecting more highly ionizing particles associated with secondary vertices. It provides an additional background reduction of about 20%. No such particles were found to be associated with the decay vertex of the first ν_τ candidate event.

The expected background in the muon decay channel caused by large-angle muon scattering has been evaluated in [9].

The total number of expected background events has slightly decreased from 0.75 as quoted in the experiment proposal [9] to 0.73, despite a significant increase of the charm cross-sections, mainly because of a significant improvement in the identification of the decay products as hadron or muon. All background sources are summarized in table 5. Systematic errors of 25% on charm background and of 50% on hadron and muon backgrounds are assumed. Errors arising from the same source are combined linearly and otherwise in quadrature.

6 Signal statistical significance

One ν_τ candidate event is observed in the $\tau \to h$ decay channel that passes all the selection cuts; assuming full mixing and $\Delta m^2_{23} = 2.5 \times 10^{-3} eV^2$ 0.49 ± 0.12 events are expected for this decay mode in the currently analysed sample. The error is estimated close to 25% from

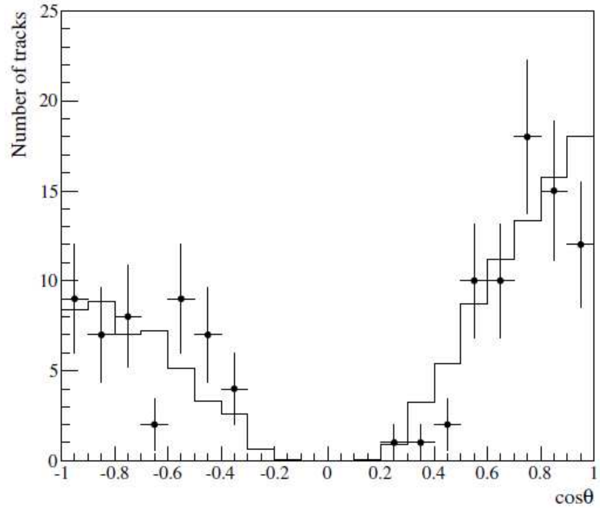

Figure 7: Polar angle distributions of the highly ionizing particles emitted in 8 GeV/c π^- interactions in an OPERA-like brick for experimental data (dots with error bars) and simulated data (histogram). Forward tracks correspond to $cos\theta = 1$.

Table 5: The expected numbers of observed background events from different sources for the design intensity of 22.5×10^{19} p.o.t. and for the 2008 and 2009 analysed data sample corresponding to 4.88×10^{19} p.o.t. Errors quoted are systematic.

Decay channel	Number of background events expected for							
	$22.5 \times 10^{19} p.o.t.$				$4.88 \times 10^{19} p.o.t.$			
	Charm	Hadron	Muon	Total	Charm	Hadron	Muon	Total
$\tau \to \mu$	0.025	0.00	0.07	0.09 ± 0.04	0.00	0.00	0.02	0.02 ± 0.01
$\tau \to e$	0.22	0.00	0.00	0.22 ± 0.05	0.05	0.00	0.00	0.05 ± 0.01
$\tau \to h$	0.14	0.11	0.00	0.24 ± 0.06	0.03	0.02	0.00	0.05 ± 0.01
$\tau \to 3h$	0.18	0.00	0.00	0.18 ± 0.04	0.04	0.00	0.00	0.04 ± 0.01
Total	0.55	0.11	0.07	0.73 ± 0.15	0.12	0.02	0.02	0.16 ± 0.03

the uncertainties on the tau production cross-section and on the detection efficiency. The background in this channel is evaluated to 0.05 ± 0.01(syst) event. The probability for the event to be not due to background fluctuations and thus the statistical significance of the observation is 95%. Considering all decay channels, the numbers of expected signal and background events are, respectively, 1.65 ± 0.41 and 0.16 ± 0.03(syst), the probability for the event to be background being 15%.

The statistical significance for the two observed events together is being estimated.

7 Electron neutrino studies

A systematic search of ν_e events in the 2008 and 2009 data was performed. A special technique was developed for ν_e search: for each located event the primary track is extrapolated to the CS where a shower search is performed. If shower-like tracks are found on the CS, an additional volume is scanned in the brick for shower search. From 505 neutral current-like events in the 2008 and 2009 data 96 events were selected using this procedure. In total 19 ν_e events were confirmed (figure 8).

The background is made by events with a γ producing an e^+e^- pair, where one of the electrons is not reconstructed. This can be the case when for example one electron has a low

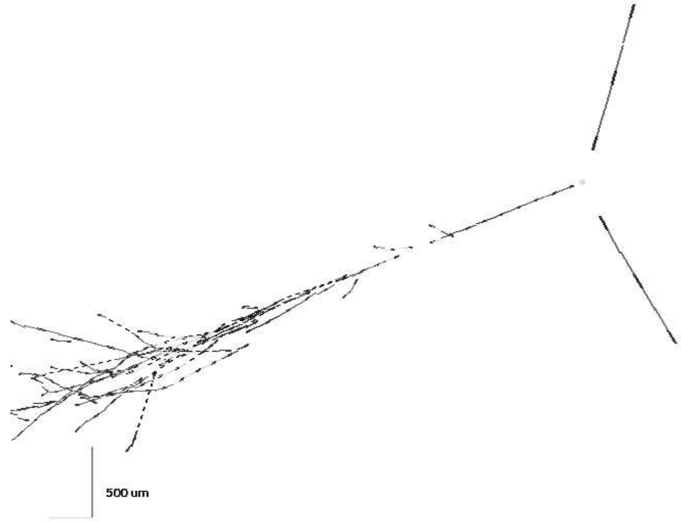

Figure 8: One of confirmed ν_e events.

energy and a strong scattering makes impossible to connect it to the pair. The total number of background in the ν_e events for 2008-2009 data is estimated to be 0.16 events. The work on efficiency estimation, tuning the total energy measurement in the electronic detector and the backgrounds estimation is still in progress.

On figure 9 predicted distributions of prompt and oscillation electron neutrino events and preliminary experimental data are given as a function of energy. The cut is set after the maximum of the beam prompt electron neutrino distribution. Number of expected ν_e beam events in this region ($E < 20$ GeV) is 3.7, oscillation ν_e events 1.1, observed in $2008 - 2009$ data 4 events. These are preliminary results and we expect to increase the total statistics by a factor of 3.

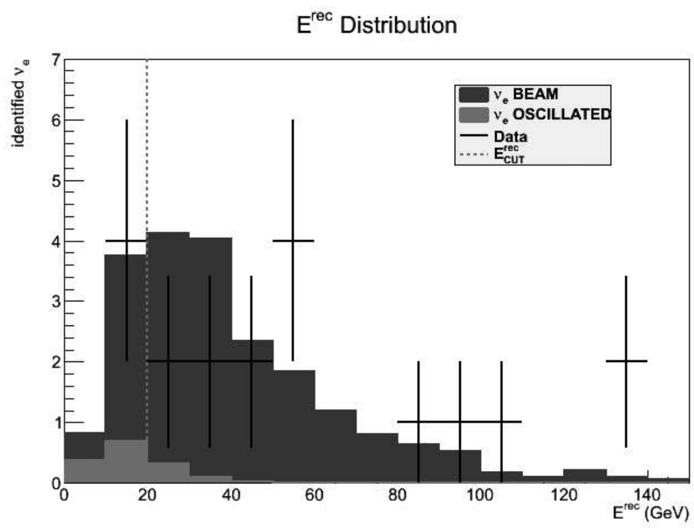

Figure 9: Distribution of expected beam and oscillated electron neutrino events as a function of energy and experimental data for the 2008-2009 sample. The selection cut at 20 GeV is shown.

8 Neutrino time of flight

In addition to the OPERA main goal, the experiment is well suited to determine the neutrino velocity with high accuracy through the measurement of the time of flight and of the distance between the source of the CNGS neutrino beam at CERN (CERN Neutrino beam to Gran Sasso) [23] and the OPERA detector at LNGS. For CNGS neutrino energies, $< E_\nu >= 17$ GeV, the relative deviation from the speed of light c of the neutrino velocity due to its finite rest mass is expected to be smaller than 10^{-19}, even assuming the mass of the heaviest neutrino eigenstate to be as large as 2 eV [24].

In the past, a high energy ($E_\nu > 30$ GeV) and short baseline experiment was able to test deviations down to $(v - c)/c < 4 \times 10^{-5}$ [25]. With a baseline analogous to that of OPERA but at lower neutrino energies (E_ν peaking at 3 GeV with a tail extending above 100 GeV), the MINOS experiment reported a measurement of $(v - c)/c = (5.1 \pm 2.9) \times 10^{-5}$ [26]. At much lower energy, in the 10 MeV range, a stringent limit of $|v - c|/c < 2 \times 10^{-9}$ was set by the observation of (anti) neutrinos emitted by the SN1987A supernova [27].

We define neutrino velocity as the ratio of the measured distance from CERN to OPERA to the time of flight of neutrinos traveling through the Earth's crust. The final result of the measurement, taking in account all systematic uncertainty is then:

$$\delta t = TOF_c - TOF_\nu = (6.5 \pm 7.4(stat.)^{+8.3}_{-8.0}(sys.))ns.$$

Delay values used for obtaining final δt are summarized in table 6.

Table 6: Summary of the time delay values used in the analysis.

	Time delay (ns)
Baseline	2439280.9
Earth rotation (Sagnac effect)	2.2
UTC corrections at CERN:	
CTRI signal propagation through GMT chain δt_{UTC}	10085.0
Kicker magnet signal to WFD $\delta t_{trigger}$	30
BCT signal to WFD δt_{BCT}	-580
UCT corrections at Gran Sasso:	
LNGS 8.3 km fiber to OPERA Master Clock	-41068.6
TT response to FPGA	59.6
FPGA latency	-24.5
Master Clock to FPGA δt_{clock}	-4262.9
GPS Corrections:	
Time-link	-2.3

This corresponds to relative difference of the muon neutrino velocity with respect to the speed of light is:

$$(v - c)/c = \delta t/(TOF'_c - \delta t) = (2.7 \pm 3.1(stat.)^{+3.4}_{-3.3}(sys.)) \times 10^{-6}$$

In performing this last calculation a baseline of 730.085 km was used, and TOF'_c corresponds to this effective neutrino baseline starting from the average meson decay point in the CNGS-CERN tunnel as determined by simulations. Actually, the δt value is measured over the distance from the BCT (Beam Current Transformer, which is placed on the proton line upstream of the CNGS target) to the OPERA reference frame, and it is essentially determined by neutrinos and not by charged pions and kaons, which introduce negligible delays.

In these calculations we used the high-statistics data taken by OPERA in the years 2009, 2010 and 2011. Dedicated upgrades of the timing systems for the time tagging and synchronization of the CNGS beam at CERN and of the OPERA detector at LNGS resulted in a reduction of the systematic uncertainties down to the level of the statistical error. The measurement also relies on a geodesy campaign that allowed measuring the 730 km CNGS baseline with a precision of 20 cm.

To exclude possible systematic effects related to the use of the proton waveforms as PDF for the distributions of the neutrino arrival times within the two extractions and to their statistical treatment, a two-week long beam test was performed at the end of 2011. A dedicated CNGS beam was generated by an SPS proton beam set up for the purpose of the neutrino velocity measurement. The modified beam consisted of a single extraction including four bunches about 3 ns long (FWHM) separated by 524 ns. With an integrated beam intensity of 4×10^{16} protons on target a total of 20 TT and 16 RPC events were retained, leading to a value of δt measured from the average of the TT distribution of (-1.9 ± 3.7) ns and (-0.8 ± 3.5) ns from the RPC, in agreement with the value of (6.5 ± 7.4) ns obtained with the main analysis. At first order, systematic uncertainties related to the bunched beam operation are equal or smaller than those affecting the result obtained with the standard CNGS beam.

The results presented in this paper were obtained by taking into account the corrections for instrumental effects discovered after the originally reported neutrino velocity anomaly [28].

9 Conclusions

The OPERA experiment, aiming at the first detection of neutrino oscillations in direct appearance mode where the oscillated neutrino is identified, completed the study of 92% of the data accumulated during the first two years of operation in the CNGS beam (2008 and 2009), corresponding to an integrated intensity of 4.88×10^{19} p.o.t.

The observation of a single candidate ν_τ event is compatible with the expectation of 1.65 signal events. The significance of the observation of one decay in the $\tau \to$ h channel decreased from 98.2% in the first analysis [12] to 95%, because of the significantly larger size of the analysed event sample.

The anticipated background increase resulting from the recently measured [21] charm cross-sections larger than those known at the time of the experimental proposal was compensated for by a higher muon identification efficiency. In addition, the study of highly ionizing tracks left by protons and nuclear fragments which are often associated with hadronic re-interactions has allowed reducing by about 20% this background specific to the hadronic decay modes of the τ.

The event location efficiency was re-evaluated for several phases of the analysis procedure. The simulation of the event reconstruction at the emulsion film level down to the interaction vertex is at an advanced stage; its completion will help in further checking the detection efficiencies at each step of the analysis process, from the track reconstruction in the electronic detectors to the location of primary and secondary vertices in the emulsion films. This will also allow re-evaluating the selection criteria in view of improving the signal-to-noise ratio.

An analysis of the large event samples collected in the 2010 and 2011 CNGS runs and corresponding to 8.88×10^{19} p.o.t. is in progress. In this sample a second ν_τ candidate event is already observed, which passes all cuts for $\tau \to h$ chanel, defined in the experiment proposal. Estimation of event's significans is going on.

An electron neutrino events search procedure was developed. 19 ν_e events were selected using it. We expect 3 times increase in electron neutrino statistics.

OPERA has reevaluated its neutrino velocity results taking in account all systematic effects. The result obtained is $\delta t = TOF_c - TOF_\nu = (6.5 \pm 7.4(stat.)^{+8.3}_{-8.0}(sys.))ns$. We have also presented the results of the bunched beam test which was performed at the end of 2011. These results are consistent with the above cited results.

References

[1] Pontecorvo B 1957 *Zh. Eksp. Teor. Fiz.* 33 549
Pontecorvo B 1957 *Sov. Phys.*JETP 6 429 (Engl. transl.)
Pontecorvo B 1958 *Zh. Eksp. Teor. Fiz.* 34 247
Pontecorvo B 1958 *Sov. Phys.JETP* 7 172 (Engl. transl.)
Maki Z, Nakagawa M and Sakata S 1962 *Prog. Theor. Phys.* 28 870

[2] Fukuda Y *et al* (SUPER-KAMIOKANDE Collaboration) 1998 *Phys. Rev. Lett.* 81 1562
Abe K *et al* (SUPER-KAMIOKANDE Collaboration) 2006 *Phys. Rev. Lett.* 97 171801
Wendell R *et al* (SUPER-KAMIOKANDE Collaboration) 2010 *Phys. Rev.* D 81 092004

[3] Nakamura K *et al* (Particle Data Group) 2010 *J. Phys.* G 37 075021

[4] Hirata K S *et al* (KAMIOKANDE-II Collaboration) 1988 *Phys. Lett.* B 205 416
Ambrosio M *et al* (MACRO Collaboration) 1998 *Phys. Lett.* B 434 451
Allison W W M *et al* (SOUDAN-2 Collaboration) 2005 *Phys. Rev.* D 72 052005

[5] Ahn M H *et al* (K2K Collaboration) 2006 *Phys. Rev.* D 74 072003
Michael D G *et al* (MINOS Collaboration) 2006 *Phys. Rev. Lett.* 97 191801
Adamson P *et al* (MINOS Collaboration) 2008 *Phys. Rev. Lett.* 101 221804

[6] Apollonio M *et al* (CHOOZ Collaboration) 2003 *Eur. Phys. J.* C 27 331
Piepke A (Palo Verde Collaboration) 2002 *Prog. Part. Nucl. Phys.* 48 113

[7] Abe K *et al* (T2K Collaboration) 2011 *Phys. Rev. Lett.* 107 041801

[8] Ereditato A, Niwa K and Strolin P 1997 The emulsion technique for short, medium and long baseline $\nu_\mu \to \nu_\tau$ oscillation experiments 423 INFN-AE-97-06, DAPNU-97-07
Shibuya H *et al* (OPERA Collaboration) 1997 Letter of intent: the OPERA emulsion detector for a longbaseline neutrino-oscillation experiment, CERN-SPSC-97-24, LNGS-LOI-8-97

[9] Guler M *et al* (OPERA Collaboration) 2000 An appearance experiment to search for $\nu_\mu \to \nu_\tau$ oscillations in the CNGS beam: experimental proposal, CERN-SPSC-2000-028, LNGS P25/2000
Guler M *et al* (OPERA Collaboration) 2001 Status Report on the OPERA Experiment, CERN/SPSC 2001-025, LNGS-EXP 30/2001 add. 1/01

[10] Elsener K 1998 The CERN Neutrino Beam to Gran Sasso (Conceptual Technical Design), CERN 98-02, INFN/AE-98/05
Bailey R *et al* 1999 The CERN Neutrino Beam to Gran Sasso (NGS) (Addendum to Report No. CERN 98-02, INFN/AE-98/05), CERN-SL/99-034(DI), INFN/AE-99/05

[11] Acquafredda R *et al* (OPERA Collaboration) 2006 *New J. Phys.* 8 303
Agafonova N *et al* (OPERA Collaboration) 2009 *J. Instrum.* 4 P06020

[12] Agafonova N *et al* (OPERA Collaboration) 2010 *Phys. Lett.* B 691 138

[13] Acquafredda R *et al* (OPERA Collaboration) 2009 *J. Instrum.* 4 P04018

[14] Armenise N *et al* 2005 *Nucl. Instrum. Methods* A 551 261
De Serio M *et al 2005 Nucl. Instrum. Methods* A 554 247
Arrabito L *et al* 2006 *Nucl. Instrum. Methods* A 568 578
Morishima K and Nakano T 2010 *J. Instrum.* 5 P04011

[15] Anokhina A *et al* (OPERA Collaboration) 2008 *J. Instrum.* 3 P07002
Anokhina A *et al* (OPERA Collaboration) 2008 *J. Instrum.* 3 P07005
Adam T *et al* 2007 *Nucl. Instrum. Methods* A 577 523
Nakamura T *et al* 2006 *Nucl. Instrum. Methods* A 556 80

[16] OPERA Collaboration 2009 OpCarac: an algorithm for the classification of the neutrino interactions recorded by OPERA *OPERA public note* 100 http://operaweb.lngs.infn.it:2080/Opera/publicnotes/note100.pdf

[17] Agafanova N *et al* (OPERA Collaboration) 2011 *New J. Phys.* 13 053051

[18] Ariga A, Ariga T, De Serio M, Di Capua F, Di Crescenzo A and Sato O 2011 The OPERA decay search procedure OPERA *public note* 128 http://operaweb.lngs.infn.it:2080/Opera/publicnotes/note128.pdf

[19] Agafanova N *et al* (OPERA Collaboration) 2011 *New J. Phys.* 14 013026

[20] OPERA Collaboration Neutrino interactions simulation in the ECC bricks of the OPERA experiment, in preparation

[21] Kayis-Topaksu A *et al* (CHORUS Collaboration) 2011 *New J. Phys.* 13 093002

[22] FLUKA http://www.fluka.org/fluka.php
Battistoni G *et al* 2007 *Proc. Hadronic Shower Simulation Workshop 2006 (Fermilab, 68 September 2006)* ed M Albrow and R Raja *AIP Conf. Proc.* 896 3149

[23] Ed. K. Elsener, *The CERN Neutrino beam to Gran Sasso* (Conceptual Technical Design), CERN98-02, INFN/AE-98/05;
R. Bailey et al., *The CERN Neutrino beam to Gran Sasso (CNGS)* (Addendum to CERN 98-02, INFN/AE-98/05), CERN-SL/99-034(DI), INFN/AE-99/05.

[24] Ch. Weinheimer et al., *Phys. Lett.* B 460 (1999) 219;
Ch. Weinheimer et al., *Phys. Lett.* B 464 (1999) 352;
M. Lobashev et al., *Phys. Lett.* B 460 (1999) 227.

[25] G. R. Kalbeisch , *Phys. Rev. Lett.* 43, 1361 (1979);
J. Alspector et al., *Phys. Rev. Lett.* 36, 837 (1976).

[26] MINOS Collaboration, P. Adamson at al., *Phys. Rev.* D 76 (2007) 072005.

[27] K. Hirata et al., *Phys. Rev. Lett.* 58 (1987) 1490;
R. M. Bionta et al., *Phys. Rev. Lett.* 58 (1987) 1494;
M. J. Longo, *Phys. Rev.* D 36 (1987) 3276.

[28] OPERA Collaboration, T. Adam et al., *Measurement of the neutrino velocity with the OPERA detector in the CNGS beam*, arXiv:1109.4897v3 [hep-ex]